Synthesis and Visualization of Densely Grafted Molecular Brushes with Crystallizable Poly(octadecyl methacrylate) Block Segments

Shuhui Qin and Krzysztof Matyjaszewski*

Center for Macromolecular Engineering, Department of Chemistry, Carnegie Mellon University, Pittsburgh, Pennsylvania 15213

Hui Xu and Sergei S. Sheiko

Department of Chemistry, University of North Carolina at Chapel Hill, Chapel Hill, North Carolina 27599-3290

Received September 12, 2002; Revised Manuscript Received December 5, 2002

ABSTRACT: Densely grafted molecular brushes with AB and ABA "block−graft" architectures, i.e., pODMA-*b*-p(BPEM-*g*-*n*BuA) and pODMA-*b*-p(BPEM-*g*-*n*BuA)-*b*-pODMA, were synthesized by the "grafting from" approach using atom transfer radical polymerization (ATRP). The backbone macroinitiators were prepared in three steps. First, ATRP of ODMA or HEMA-TMS was carried out from mono- or difunctional initiators to form macroinitiators, followed by ATRP of HEMA-TMS or ODMA initiated from these macroinitiators to obtain pODMA-*b*-pHEMA-TMS or pODMA-*b*-pHEMA-TMS-*b*-pODMA macromolecular backbone precursors. Finally, these precursors were esterified to pODMA-*b*-pBPEM and pODMA-*b*-pBPEM-*b*-pODMA backbone macroinitiators. The p*n*BuA side chains were grafted from the pBPEM segments of these backbone macroinitiators by ATRP. AFM measurement of the final molecular brushes demonstrated that the backbone of the brushes, the pBPEM segment, was almost completely stretched on the mica surface. pODMA segments tended to associate, due to crystallization of the relatively long C18 chains, and form "dimers" for AB block brushes and "multimers" or "circles" for ABA block brushes.

Introduction

Densely grafted copolymers, i.e., molecular brushes, have recently received considerable attention.[1−4] Typically, the molecular brushes are synthesized by conventional radical polymerization of macromonomers, prepared by ionic, group transfer, or ring-opening metathesis polymerization.[5] These polymerization methods limit the range of monomers that can be used for macromonomer synthesis. However, conventional free radical polymerization cannot control the degree of polymerization of the final brushes.

Controlled/living radical polymerization produces polymers with controlled molecular weight and narrow molecular weight distributions and with various architectures.[6−9] Atom transfer radical polymerization (ATRP) is among the most efficient methods and has been applied to a large range of vinyl monomers, including styrene, (meth)acrylates, and acrylonitrile to form linear, (hyper)branched, comblike, and starlike structures.[9−15] So far, ATRP has been used successfully to prepare molecular brushes with either methacrylate or polystyrene backbones and various polyacrylates and polymethacrylate and poly(ethylene oxide) side chains.[16−21] In addition, side chains with block copolymer structures have been prepared.[17,19] The length of the main chain has been varied from $DP_{MC} = 100$ to 4000 and side chains from $DP_{SC} < 10$ to ∼100.

Homopolymers and copolymers of poly(octadecyl acrylate) (pODA) and poly(octadecyl methacrylate) (pODMA) have been studied extensively due to their interesting bulk and solution properties. Cooperative organization of the long side chains enables these polymers to crystallize, despite the atacticity of the main chains.[22,23] Both conventional radical polymerization and anionic polymerization of ODMA yielded polymers with poorly controlled structures.[24,25] Therefore, a major challenge is to prepare well-defined (co)polymers with poly(octadecyl) segments. We recently used ATRP to successfully synthesize well-defined homopolymers, block, statistical, and gradient copolymers containing poly(dodecyl acrylate) and also pODMA and pODA.[26,27]

Here we report the synthesis of densely grafted molecular brushes pODMA-*b*-p(BPEM-*g*-*n*BuA) and pODMA-*b*-p(BPEM-*g*-*n*BuA)-*b*-pODMA in which pODMA chains were introduced at one or both ends of cylindrical brush molecules. Individual molecules, including backbones, p*n*BuA side chains, and pODMA tails, were visualized by AFM. The results demonstrate that the backbone of the brushes is almost completely stretched on the mica surface, while ODMA blocks tend to associate to form "dimers" for AB block brushes and "multimers" for ABA block brushes.

Experimental Section

Materials. Octadecyl methacrylate (ODMA) (Polysciences Inc., 99%) was purified by dissolution in hexane and extraction four times with 5% aqueous NaOH. After drying the organic phase over anhydrous magnesium sulfate, the solution was passed through neutral alumina and solvent was removed under reduced pressure. 2-(Trimethylsilyloxyl)ethyl methacrylate (HEMA-TMS) was synthesized according to a literature procedure.[28] *n*-Butyl acrylate (*n*BuA) (Aldrich, 98%) was dried over calcium hydride and then distilled under reduced pressure. Ethyl 2-bromoisobutyrate (Acros, 98%) and dimethyl 2,6-dibromoheptanedioate (DMDBH) (Aldrich, 97%) were used as received. Copper(I) bromide (Cu(I)Br) (Acros, 98%) and copper(I) chloride (Cu(I)Cl) (Acros, 99%) were purified by washing with glacial acetic acid, followed by absolute ethanol and acetone, and then dried under vacuum. Copper(II) bromide ($Cu(II)Br_2$) (Aldrich, 99%) and copper(II) chloride ($Cu(II)Cl_2$) (Aldrich, 99+%) were used as received. 4,4′-Di(5-nonyl)-2,2′-bipyridine (dNbpy) was prepared as described elsewhere.[29] All

10.1021/ma021472w CCC: $25.00
Published on Web 01/16/2003

other regents and solvents were used as received from Aldrich or Acros Chemicals.

Measurements. Monomer conversion of HEMA-TMS and *n*BuA was determined using a Shimadzu GC 14-A gas chromatograph (GC) equipped with a FID detector using a J&W Scientific 30 m DB WAX Megabore column. Injector and detector temperatures were kept constant at 250 °C; the column was heated from 40 to 160 °C with a heating rate of 20 °C/min. Monomer conversion of ODMA and (co)polymer composition was analyzed by ^{1}H NMR in $CDCl_3$ on a Bruker 300 MHz instrument. Elemental analysis was done at Midwest Microlab, LLC. (Co)polymer molecular weights were determined at 35 °C using a GPC system equipped with a Waters WISP 712 autosampler and Polymer Standards Service columns (guard, 10^2, 10^3, and 10^5 Å). Tetrahydrofuran (THF) was used as eluant with a rate of 1 mL/min, and toluene was used as an internal standard for the system. Atomic force micrographs were obtained using a Multimode Nanoscope IIIa instrument (Digital Instruments-Veeco Metrology Group, St. Barbara, CA) operating in the tapping mode. The measurements were performed at ambient conditions using Si cantilevers with a spring constant of ca. 50 N/m and a resonance frequency of about 300 kHz. The set-point amplitude ratio was maintained at 0.9 to minimize the sample deformation induced by the tip. The samples for tapping mode AFM measurements were prepared by spin-casting on a rotating substrate at 2000 rpm of dilute solutions of brush molecules in chloroform.

Polymer Synthesis. I. pODMA-*b*-*p*(BPEM-*g*-*n*BuA) Molecular Brushes. Synthesis of pODMA-*b*-pBPEM Backbone Macroinitiator. The AB type block copolymer with the ATRP initiators in one block segment (pODMA-*b*-pBPEM) was synthesized via the following three steps.

Synthesis of pODMA Macroinitiator. In a 25 mL dried Schlenk flask, Cu(II)Cl_2 (1.3 mg, 0.01 mmol) and dNbpy (163.5 mg, 0.4 mmol) were purged three times with inert gas. Deoxygenated OMA (6.77 g, 20 mmol) and 8 mL of *o*-xylene were then added, and the reaction mixture was degassed by three freeze−pump−thaw cycles. After stirring for 1 h at room temperature (rt), Cu(I)Cl (19.8 mg, 0.2 mmol) was added, and the flask was placed in a thermostated oil bath at 90 °C. After 3 min, ethyl 2-bromoisobutyrate (29.3 μL, 0.2 mmol) was injected and an initial kinetic sample was taken. During the polymerization, samples were removed to analyze conversion by ^{1}H NMR and analyze molecular weight by GPC. After 8 h, the polymerization was stopped at 92% conversion by cooling to rt and opening the flask to air. The mixture was then dissolved into 40 mL of THF, passed through a neutral alumina column, and precipitated into 600 mL of methanol. The obtained polymer was then collected in a Buchner funnel washed with a large quantity of acetone in order to remove the unreacted ODMA monomer. pODMA macroinitiator with $M_n = 3.47 \times 10^4$ ($M_w/M_n = 1.12$) was successfully synthesized.

Synthesis of pODMA-b-pHEMA-TMS. In a 25 mL Schlenk flask, $CuCl_2$ (0.13 mg, 0.001 mmol in stock solution), pODMA (0.708 g, 0.02 mmol), and dNbpy (16.4 mg, 0.04 mmol) were purged three times with inert gas. Deoxygenated HEMA-TMS (1.62 g, 8.0 mmol) and 2 mL of *o*-xylene were then added, and the reaction mixture was degassed by three freeze−pump−thaw cycles. After stirring for 1 h at rt, CuCl (1.98 mg, 0.02 mmol) was added, and the flask was placed in a thermostated oil bath at 85 °C. After 3 min, an initial kinetic sample was taken, and samples were removed to analyze conversion by GC using *o*-xylene as internal standard and analyze molecular weight by GPC during the polymerization. After 94 h, the polymerization was stopped at 73.1% conversion by cooling to rt and opening the flask to air. The mixture was then dissolved into 40 mL of THF and passed through a neutral alumina column, and the solvent and the residual monomer were removed via high vacuum. The molecular weight and molecular weight distribution of the resultant pODMA-*b*-pHEMA-TMS were $M_n = 7.45 \times 10^4$ and $M_w/M_n = 1.23$, respectively.

Synthesis of pODMA-b-pBPEM. The product of the pODMA-*b*-HEMA-TMS copolymer was placed in a 250 mL round-bottom flask (assuming 5.85 mmol of R−OTMS groups). After KF (0.34 g, 5.85 mmol) addition, the flask was sealed and flushed with N_2, and 100 mL of dry THF was added. Tetrabutylammonium fluoride (0.0157 g, 0.06 mmol) was added dropwise to the flask, followed by the slow addition of 2-bromopropionyl bromide (1.90 g, 0.92 mL, 8.80 mmol) over the course of 30 min. The reaction mixture was stirred at rt for 4 h and then precipitated into a mixture of methanol/ice (80/20 v/v %). The precipitate was redissolved in 150 mL of $CHCl_3$ and filtered through a column of basic activated alumina, and the solvent was removed on a rotary evaporator. The isolated polymer was reprecipitated from THF into hexanes twice and dried under vacuum at 25 °C for 24 h; 1.2 g of pODMA-*b*-pBPEM was obtained (53% yield). The conversion was complete according to the absence of TMS−O− resonance ($\delta = 0.2$ ppm (9H, bs, $(H_3C)_3Si-$)) in the ^{1}H NMR spectrum. M_n(GPC) $= 7.52 \times 10^4$; $M_w/M_n = 1.17$. ^{1}H NMR (δ in ppm): pBPEM part: 4.52 (1H, quart., $J = 6.8$ Hz, Br−C*H*−CH_3); 4.36 (2H, bs, −O−CH_2−C*H*$_2$−O−CO−CH−Br); 4.15 (2H, bs, −O−C*H*$_2$−CH_2−O−CO−CH−Br); 1.82 (overlapped, d, $J = 6.8$ Hz, Br−CH−C*H*$_3$); 2.21−1.44 (overlapped, m, C*H*$_2$−C−CH_3); 1.22−0.94 (overlapped, 3 × bs, CH_2−C−C*H*$_3$). pODMA part: 3.85 (2H, bs, −O−C*H*$_2$(C*H*$_2$)$_{16}$C*H*$_3$); 1.39−1.11 (overlapped, bs, −CH_2-(C*H*$_2$)$_{16}$C*H*$_3$); 1.51−1.39 (overlapped, 3 × bs, CH_2(C*H*$_2$)$_{16}$C*H*$_3$); 2.11−1.37 (overlapped, m, CH_3−C−C*H*$_2$); 1.37−0.75 (overlapped, 3 × bs, C*H*$_3$−C−CH_2). Overall ratio [BPEM]:[ODMA] (^{1}H NMR) = 77:23. Elem Anal. Found (calcd) for pODMA-*b*-pBPEM: C, 51.52 (51.63); H, 7.19 (7.14); Br, 20.49 (21.54). Overall ratio [BPEM]:[ODMA] (Elem Anal.) = 74:26.

pODMA-*b*-p(BPEM-*g*-*n*BuA). In a 100 mL Schlenk flask pODMA-*b*-pBPEM (0.1 g, 0.2 mmol initiating sites (based on ^{1}H NMR result)), $CuBr_2$ (1.12 mg, 0.005 mmol in stock solution), and dNbpy (81.6 mg, 0.2 mmol) were purged three times with inert gas. Deoxygenated *n*BuA (12.8 g, 0.1 mol) and anisole (3.5 mL, 25 vol %) were added, and the reaction mixture was degassed by three freeze−pump−thaw cycles. After stirring for 1 h at rt, CuBr (14.34 mg, 0.1 mmol) was added, and the flask was placed in a thermostated oil bath at 70 °C. After 3 min, an initial kinetic sample was taken, and samples were removed to analyze conversion by GC using anisole as internal standard and analyze molecular weight by GPC during the polymerization. The polymerization was stopped at 6.8% conversion after 33 h by cooling to rt and opening the flask to air. The polymer was purified by distilling off both the solvent and the monomer under high vacuum at room temperature, dissolving the crude polymer in methylene chloride (about 100 mL), and passing it through an alumina column, followed by removing the solvent on a rotary evaporator (25 °C) and drying the product in high vacuum at room temperature for 24 h. Yield: 0.99 g of isolated polymer ($DP_{sc,grav} = 35$). The detailed analytic results are listed in Table 1.

Table 1. Data for pODMA-*b*-p(BPEM-*g*-*n*BuA) Molecular Brushes Synthesis

polymer	$M_{n,\,app}$	M_w/M_n	DP_n
pODMA	3.47×10^4	1.12	92
pODMA-*b*-pHEMA-TMS	7.45×10^4	1.23	92/292
pODMA-*b*-pBPEM	7.52×10^4	1.17	92/292
pODMA-*b*-p(BPEM-*g*-*n*BuA)	4.09×10^5	1.27	92/292*35

II. pODMA-*b*-p(BPEM-*g*-*n*BuA)-*b*-pODMA Molecular Brushes. Synthesis of pODMA-*b*-pBPEM-*b*-pODMA Backbone Macroinitiator. The ABA type block copolymer with the ATRP initiators in the center block, pODMA-*b*-pBPEM-*b*-pODMA, was synthesized using a similar procedure to that of pODMA-*b*-pBPEM.

Synthesis of Difunctional pHEMA-TMS Macroinitiator. In a 25 mL dried Schlenk flask Cu(II)Br_2 (1.84 mg, 0.00824 mmol) and dNbpy (134.4 mg, 0.329 mmol) were purged three times with inert gas. Deoxygenated HEMA-TMS (5.0 g, 24.7 mmol) and anisole (1.1 mL, 20 vol %) were added; the reaction mixture was degassed by three freeze−pump−thaw cycles. After stirring for 1 h at rt, CuBr (23.6 mg, 0.165 mmol) was added, and the flask was placed in a thermostated oil bath at 85 °C. After 3 min, DMDBH (17.9 μL, 0.0824 mmol) was injected, and an initial kinetic sample was taken. During the polymerization, samples were removed to analyze conversion

by GC using anisole as the internal standard and analyze molecular weight by GPC. After 3.5 h, the polymerization was stopped at 78% conversion by cooling to rt and opening the flask to air. The mixture was then dissolved into 25 mL of THF and passed through neutral alumina column, and the solvent and the residual monomer were removed via high vacuum. The obtained pHEMA-TMS with $M_n = 5.24 \times 10^4$ ($M_w/M_n = 1.30$) was used as a difunctional macroinitiator for ABA triblock copolymer synthesis.

Synthesis of pODMA-b-pHEMA-TMS-b-pODMA. In a 25 mL Schlenk flask, $CuBr_2$ (1.60 mg, 0.0072 mmol), difunctional pHEMA-TMS macroinitiator (3.60 g, 0.07 mmol), and dNbpy (114 mg, 0.28 mmol) were purged three times with inert gas. Deoxygenated OMA (14.0 g, 41.4 mmol) and 11 mL of *o*-xylene were then added, and the reaction mixture was degassed by three freeze−pump−thaw cycles. After stirring for 1 h at rt, CuBr (20 mg, 0.14 mmol) was added, and the flask was placed in a thermostated oil bath at 90 °C. After 3 min, an initial kinetic sample was taken, and samples were removed to analyze conversion by ^{1}H NMR and analyze molecular weight by GPC during the polymerization. After 7.0 h, the polymerization was stopped at 76% conversion by cooling to rt and opening the flask to air. The mixture was then dissolved into 25 mL of THF and passed through a neutral alumina column, and the solvent was removed via high vacuum (the residual OMA monomer can be removed after esterification). The macroinitiator precursor pODMA-*b*-pHEMA-TMS-*b*-pODMA with $M_n = 1.39 \times 10^5$ ($M_w/M_n = 1.33$) was obtained.

Synthesis of pODMA-b-pBPEM-b-pODMA. The product of the pODMA-*b*-HEMA-TMS-*b*-pODMA copolymer was placed in a 250 mL round-bottom flask (assuming 17.8 mmol of R−OTMS groups). After KF (1.03 g, 17.8 mmol) addition, the flask was sealed and flushed with N_2, and 200 mL of dry THF was added. Tetrabutylammonium fluoride (0.047 g, 0.18 mmol) was added dropwise to the flask, followed by the slow addition of 2-bromopropionyl bromide (5.76 g, 26.7 mmol) over 40 min. The reaction mixture was stirred at room temperature for 4 h and afterward precipitated into a mixture of methanol/ice (80/20 v/v %). The precipitate was redissolved in 300 mL of $CHCl_3$ and filtered through a column of basic activated alumina, and the solvent was removed on a rotary evaporator. The isolated polymer was reprecipitated from THF into methanol four times to remove the remained ODMA monomer and dried under vacuum at 25 °C for 24 h; 6.5 g of pODMA-*b*-pBPEM-*b*-pODMA) was obtained (42.3% yield). The conversion was complete according to the absence of TMS−O− resonance (δ = 0.2 ppm (9H, bs, $(H_3C)_3Si-$)) in the ^{1}H NMR spectrum. M_n-(GPC) = 141 000; $M_w/M_n = 1.30$. ^{1}H NMR (δ in ppm): pBPEM part: 4.52 (1H, q, $J = 6.8$ Hz, Br−C*H*-CH_3); 4.36 (2H, bs, −O−CH_2−CH_2−O−CO−CH−Br); 4.15 (2H, bs, −O−CH_2−CH_2−O−CO−CH−Br); 1.82 (overlapped, d, $J = 6.8$ Hz, Br−CH−CH_3); 2.21−1.44 (overlapped, m, CH_2−C−CH_3); 1.22−0.94 (overlapped, 3 × bs, CH_2−C−CH_3). pODMA part: 3.85 (2H, bs, −O−CH_2(CH_2)$_{16}CH_3$); 1.39−1.11 (overlapped, bs, −CH_2(CH_2)$_{16}$-CH_3); 1.51−1.39 (overlapped, 3 × bs, CH_2(CH_2)$_{16}CH_3$); 2.11−1.37 (overlapped, m, CH_3−C−CH_2); 1.37−0.75 (overlapped, 3 × bs, CH_3−C−CH_2). Overall ratio [BPEM]:[ODMA] (^{1}H NMR) = 36:64. Elem Anal. Found (calcd) for pODMA-*b*-pBPEM-*b*-pODMA: C, 67.40 (66.72); H, 10.35 (10.21); Br, 8.68 (9.23). Overall ratio [BPEM]:[ODMA] (Elem Anal.) = 34:66.

pODMA-*b*-p(BPEM-*g*-*n*BuA)-*b*-pODMA. In a 100 mL Schlenk flask, pODMA-*b*-pBPEM-*b*-pODMA (0.245 g, 0.284 mmol initiating sites (based on ^{1}H NMR results conversion)), $CuBr_2$ (1.66 mg, 0.00743 mmol in stock solution), and dNbpy (115.8 mg, 0.283 mmol) were purged three times with inert gas. Deoxygenated *n*BuA (21.7 g, 0.17 mol) and anisole (6.1 mL, 25 vol %) were added, and the reaction mixture was degassed by three freeze−pump−thaw cycles. After stirring for 1 h at rt, CuBr (20.37 mg, 0.142 mmol) was added, and the flask was placed in a thermostated oil bath at 70 °C. After 3 min, an initial kinetic sample was taken, and samples were removed to analyze conversion by GC using anisole as internal standard and analyze molecular weight by GPC during the polymerization. The polymerization was stopped at 7.6% after 62 h by cooling to rt and opening the flask to air. The purification procedure of the polymer was the same as that with pODMA-*b*-p(BPEM-*g*-*n*BuA). Yield: 1.9 g of isolated polymer ($DP_{sc,grav} = 46$). The detailed analytic data are included in Table 2.

Table 2. Data for pODMA-*b*-p(BPEM-*g*-*n*BuA)-*b*-pODMA Molecular Brushes Synthesis

polymer	$M_{n,app}$	M_w/M_n	DP_n
pHEMA-TMS	5.24×10^4	1.30	234
pODMA-*b*-pHEMA-TMS-*b*-pODMA	1.39×10^5	1.33	205/234/205
pODMA-*b*-pBPEM-*b*-pODMA	1.41×10^5	1.30	205/234/205
pODMA-*b*-p(BPEM-*g*-*n*BuA)-*b*-pODMA	5.94×10^5	1.32	205/234*46/205

Results and Discussion

Synthesis of pODMA-*b*-(pBPEM-*g*-*n*BuA) Molecular Brushes. Densely grafted molecular brushes pODMA-*b*-(pBPEM-*g*-*n*BuA) were synthesized by grafting *n*BuA from the initiating groups of a pODMA-*b*-pBPEM backbone macroinitiator using ATRP. pODMA-*b*-pBPEM was obtained by esterification of pODMA-*b*-pHEMA-TMS macroinitiator precursor which can be synthesized either by chain extension of HEMA-TMS from pODMA macroinitiator or by chain extension of ODMA from pHEMA-TMS macroinitiator. Considering the easier purification of pODMA macroinitiator than that of pHEMA-TMS, the backbone macroinitiator pODMA-*b*-pBPEM was synthesized from ODMA as the first block (Scheme 1A).

We used the catalyst system of CuCl, $CuCl_2$, and dNbpy in a solution of *o*-xylene at 90 °C for the homopolymerization of ODMA. Ethyl 2-bromoisobutyrate (EBiB) was used as the initiator. The "halogen exchange" technique improved the control of the ATRP of ODMA.[30,31] The polymerization was stopped after 8 h, and the monomer conversion was 92% by ^{1}H NMR. The kinetics of the polymerization and evolution of M_n and M_w/M_n with monomer conversion are presented in Figure 1. The semilogarithmic kinetic plot is linear and passes through the origin, demonstrating that the number of active propagating species is constant throughout the polymerization. It also indicates that the kinetics is first order in monomer concentration. The molecular weights measured by GPC increase linearly with monomer conversion and are close to the theoretical predictions ($M_{n,th}$ = conversion × MW_{ODMA} × $[ODMA]_0/[EBiB]_0$). The slightly systematically higher $M_{n,GPC}$ compared to $M_{n,th}$ might be due to the hydrodynamic volume differences between pODMA polymers and pMMA standards. In addition, the polydispersity of the polymers is low in all cases ($M_w/M_n = 1.12$ at 92% conversion). The results reveal that the ATRP of ODMA in macroinitiator synthesis is a controlled/living process.

Chain extension from pODMA macroinitiator by HEMA-TMS was conducted via ATRP at 85 °C. It required higher dilution of macroinitiator in *o*-xylene relative to the HEMA-TMS homopolymerization to avoid the effect of long bulky C18 side chain on the initiation efficiency of the Cl end groups, and the reaction temperature was lower than that of pODMA macroinitiator synthesis (90 °C) to improve control of the block copolymerization. The monomer conversion reached 73% after 94 h, and pODMA-*b*-pHEMA-TMS copolymer with $M_n = 7.42 \times 10^4$ and $M_w/M_n = 1.23$ was obtained. The GPC traces shown in Figure 2 revealed a shift in elution volume of block copolymer from that of

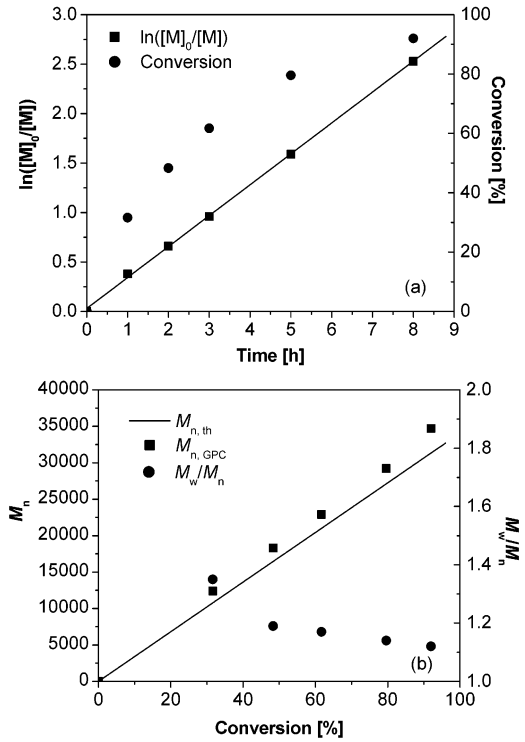

Figure 1. (a) Dependence of $\ln([M]_0/[M])$ and conversion on time in the polymerization of ODMA in *o*-xylene at 90 °C. (b) Dependence of M_n and M_w/M_n of pODMA on conversion. Conditions: $[ODMA]_0 = 2.5$ M, $[CuCl]_0 = 25$ mM, $[CuCl_2]_0 = 1.25$ mM, $[dNbpy]_0 = 50$ mM, $[EBiB]_0 = 25$ mM.

the original pODMA macroinitiator, indicating an increase in molecular weight of the resulting block copolymer. However, there is a long tailing in the GPC traces of the block copolymer, which broadened the molecular weight distribution of the final block copolymer. This may due to residual pODMA homopolymer (i.e., dead chains), which are removed after esterification

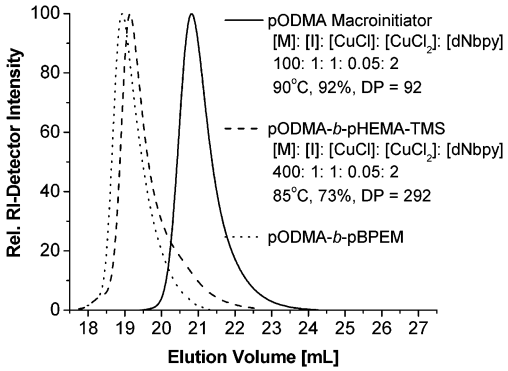

Figure 2. GPC traces during the syntheses of pODMA-*b*-pBPEM backbone macroinitiator.

by precipitating the final pODMA-*b*-pBPEM product into hexanes (pODMA dissolves well in hexanes).

The esterified block copolymer (pODMA-*b*-pBPEM) was characterized by GPC, ^{1}H NMR, and elemental analysis. The GPC results are relative pMMA (Table 1). The GPC traces shifted entirely to high molecular weight as shown in the overlaid traces of starting material and isolated product (Figure 2). There is no significant tailing or shoulder, indicating negligible contributions of side reactions and a successful removal of the residual pODMA dead chains. Therefore, the polydispersity of pODMA-*b*-pBPEM decreased ($M_n = 7.52 \times 10^4$, $M_w/M_n = 1.17$). The ^{1}H NMR spectrum confirmed the complete transformation of pHEMA-TMS segments to pBPEM segments (absence of Me_3Si- signals) and gave the molar ratio of [BPEM]:[ODMA] = 77:23. The value was close to the elemental analysis result ([BPEM]:[ODMA] = 74:26) and theoretical result ([BPEM]:[ODMA] = 76:24) which was determined by monomer conversion. The DP_n of BPEM and ODMA was 292 and 92, respectively, as summarized in Table 1.

The AB "block−graft" molecular brush was synthesized by grafting *n*BuA from pODMA-*b*-pBPEM macro-

Scheme 1. Synthesis of pODMA-*b*-pBPEM (A) and pODMA-*b*-pBPEM-*b*-pODMA (B) Macroinitiators

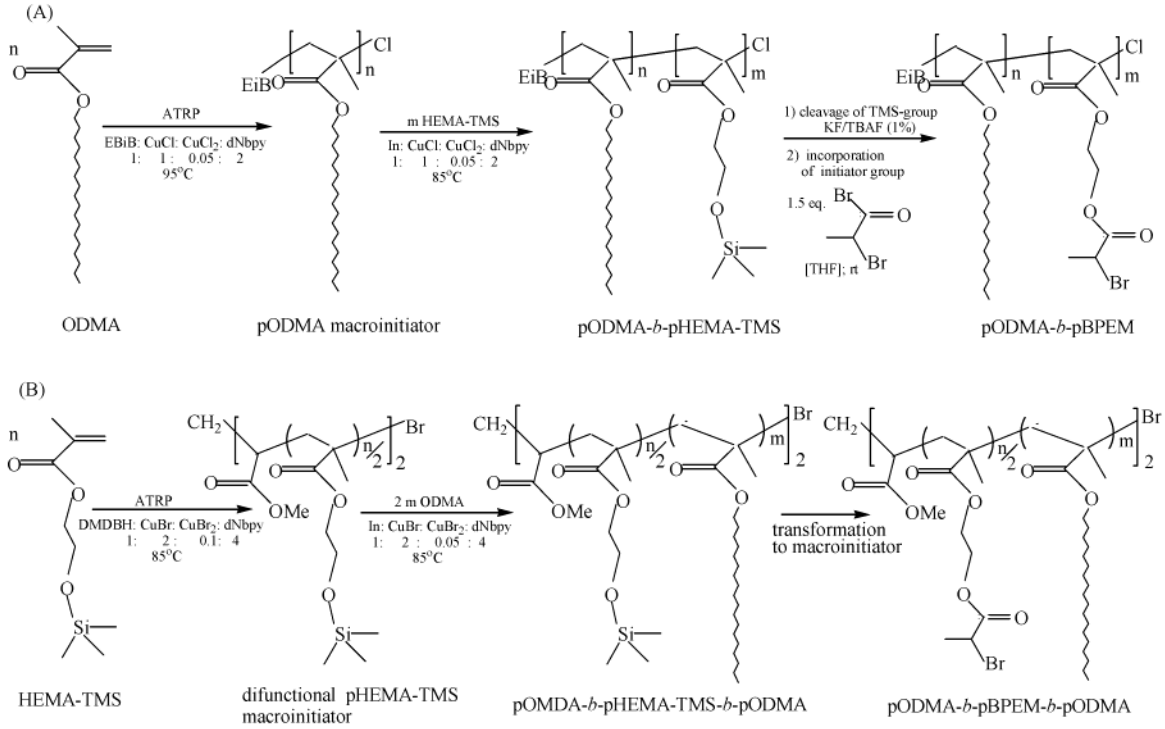

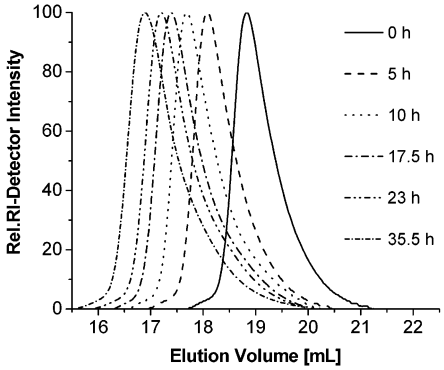

Figure 3. GPC traces during the syntheses of pODMA-*b*-p(BPEM-*g*-*n*BuA) brushes (5−33 h) from pODMA-*b*-pBPEM backbone (0 h). Conditions: $[n\text{BuA}]_0 = 5.6$ M, $[\text{CuBr}]_0 = 5.6$ mM, $[\text{CuBr}_2]_0 = 0.28$ mM, $[\text{dNbpy}]_0 = 11.2$ mM, $[\text{BPEM}]_0 = 11.2$ mM.

Scheme 2. Synthesis of pODMA-*b*-p(BPEM-*g*-*n*BuA) (A) and pODMA-*b*-p(BPEM-*g*-*n*BuA)-*b*-pODMA (B) Molecular Brushes

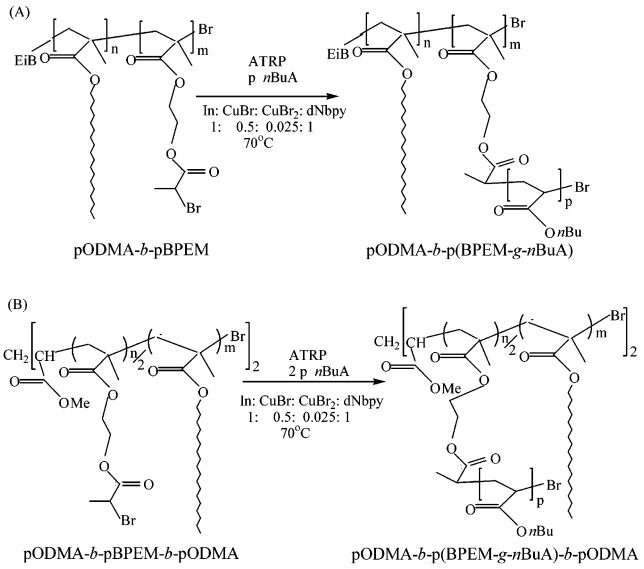

initiator (Scheme 2 A). As shown in Figure 3, the GPC traces shift continuously toward higher molecular weight throughout the polymerization. No high molecular weight shoulder was observed by comparison with that of macroinitiator (0 h), showing no evidence for brush−brush coupling. The apparent molecular weight (based on pMMA standards) increased to $M_{n,app} = 4.09 \times 10^5$ for the final pODMA-*b*-p(BPEM-*g*-*n*BuA) brushes, and the molecular weight distribution was relatively low ($M_w/M_n = 1.27$), indicating that the polymerization was controlled. The DP_n of p*n*BuA side chains was 35 by gravimetry and 36 by GC (monomer conversion).

Synthesis pODMA-*b*-(pBPEM-*g*-*n*BuA)-*b*-pODMA Molecular Brushes. Similarly, pODMA-*b*-p(BPEM-*g*-*n*BuA)-*b*-pODMA brushes were synthesized by grafting *n*BuA from pODMA-*b*-pBPEM-*b*-pODMA macroinitiator. The backbone macroinitiator was synthesized by ATRP of HEMA-TMS using a difunctional initiator, dimethyl 2,6-dibromoheptanedioate (DMDBH), followed by chain extension of ODMA from the resultant difunctional pHEMA-TMS macroinitiator and esterification of the backbone macroinitiator precursor with 2-bromopropionyl bromide (Scheme 1B).

HEMA-TMS was polymerized in anisole with CuBr/$CuBr_2$/dNbpy catalyst system at 85 °C. The first-order

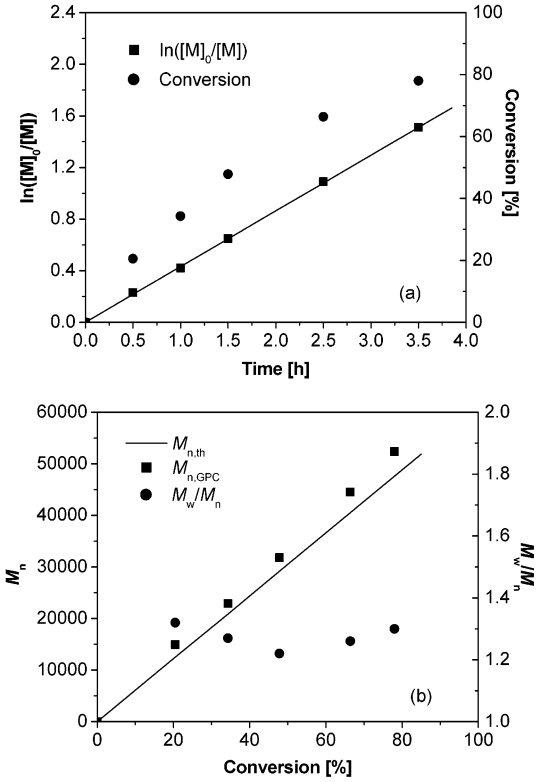

Figure 4. (a) Dependence of $\ln([M]_0/[M])$ and conversion on time in the polymerization of HEMA-TMS in anisole at 85 °C. (b) Dependence of M_n and M_w/M_n of pHEMA-TMS on conversion. Conditions: $[\text{HEMA-TMS}]_0 = 4.3$ M, $[\text{CuBr}]_0 = 28.7$ mM, $[\text{CuBr}_2]_0 = 1.44$ mM, $[\text{dNbpy}]_0 = 57.4$ mM, $[\text{DMDBH}]_0 = 14.4$ mM.

kinetic plot is shown in Figure 4a. The linear correlation of $\ln([M]_0/[M])$ vs time indicates that the concentration of growing radicals is constant throughout the polymerization. Figure 4b shows that the M_n values (measured by GPC with pMMA standards) increase linearly with increasing monomer conversion; the values are similar to the theoretical predictions calculated from the equation $M_{n,th} = \text{conversion} \times MW_{\text{HEMA-TMS}} \times [\text{HEMA-TMS}]_0/[\text{DMDBH}]_0$). Similar to the ODMA homopolymerization, the slightly systemically higher values of M_n by GPC compared to $M_{n,th}$ may be due to the hydrodynamic volume differences between the pHEMA-TMS polymers and pMMA standards. The molecular weight distributions decrease during the polymerization and are relatively narrow for the final product ($M_n = 5.24 \times 10^4$, $M_w/M_n = 1.30$). This supports the controlled/living behavior for the ATRP of HEMA-TMS.

The backbone macroinitiator precursor pODMA-*b*-pHEMA-TMS-*b*-pODMA was synthesized by chain extension of ODMA from the difunctional pHEMA-TMS macroinitiator using ATRP in *o*-xylene at 90 °C. The polymerization proceeded to 76% conversion after 7 h, and the GPC curve shifted to high molecular weight position as shown in Figure 5. The detailed results of both the starting difunctional macroinitiator and the final obtained triblock copolymer are compiled in Table 2, which shows the successful synthesis of the backbone macroinitiator precursor.

Using a similar synthetic approach as that described for pODMA-*b*-pBPEM, pODMA-*b*-pHEMA-TMS-*b*-pODMA was esterified to generate pODMA-*b*-pBPEM-*b*-pODMA backbone macroinitiator. The GPC traces shifted entirely to high molecular weight as shown in Figure

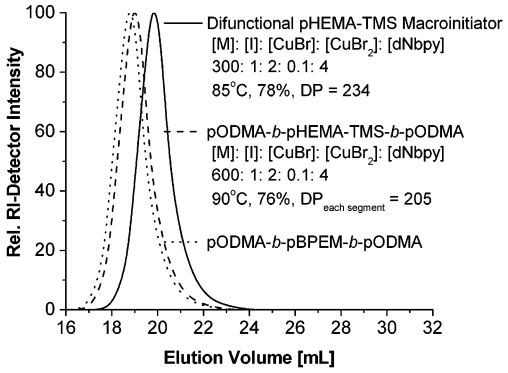

Figure 5. GPC traces during the syntheses of pODMA-*b*-pBPEM-*b*-pODMA backbone macroinitiator.

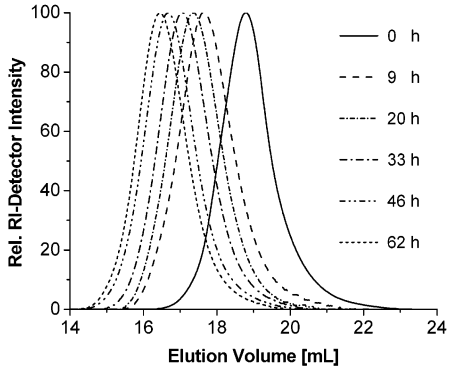

Figure 6. GPC traces during the syntheses of pODMA-*b*-p(BPEM-*g*-*n*BuA)-*b*-pODMA brushes (9−62 h) from pODMA-*b*-pBPEM-*b*-pODMA backbone (0 h). $[n\text{BuA}]_0 = 5.6$ M, $[\text{CuBr}]_0 = 4.7$ mM, $[\text{CuBr}_2]_0 = 0.24$ mM, $[\text{dNbpy}]_0 = 9.3$ mM, $[\text{BPEM}]_0 = 9.4$ mM.

5, in which there is no shoulder, indicating negligible contributions of side reactions. The average molecular weight and molecular weight distribution of the final pODMA-*b*-pBPEM-*b*-pODMA backbone macroinitiator are $M_n = 1.41 \times 10^5$ and $M_w/M_n = 1.30$ relative to pMMA standards, respectively, as summarized in Table 2. ^{1}H NMR spectroscopy showed that no Me_3Si- group was left, and the molar ratio of [BPEM]:[ODMA] = 36:64. The values given by the elemental analysis and by monomer conversion are [BPEM]:[ODMA] = 34:66 and 36:64, respectively. They fit well within the experimental error. The DP_n is 234 for the BPEM segment and 205 for each ODMA segment as summarized in Table 2.

The polymerization of *n*BuA was initiated with the well-defined pODMA-*b*-pBPEM-*b*-pODMA macroinitiator, and the polymerization resulted in an ABA "block−graft" molecular brushes pODMA-*b*-(pBPEM-*g*-p*n*BuA)-*b*-pODMA as shown in Scheme 2B. Figure 6 shows the continuous shifting of GPC traces toward higher molecular weight throughout the polymerization with no shoulder, showing the successful synthesis of the brushes and no evidence for brush−brush coupling during the polymerization. The apparent molecular weight (based on pMMA standards) was $M_{n,app} = 5.94 \times 10^5$, and M_w/M_n was 1.32 for the final pODMA-*b*-p(BPEM-*g*-*n*BuA)-*b*-pODMA brushes. The DP_n of p*n*BuA side chains is 46 by gravimetry and 48 by GC.

Atomic Force Microscopy (AFM) Characterization. Previous studies showed that molecular brushes could be visualized as single molecules by AFM.[1,32] Even the backbone and the side chains were clearly observed due to the high spatial resolution and strong material contrast of tapping mode AFM.[1,32] The monomolecular films for AFM studies were prepared by spin-casting the dilute solution of the brushes onto mica surface. In this study, because of the specific interaction and likely crystallization of the pODMA tails, brush molecules may associate to form clusters of several molecules.

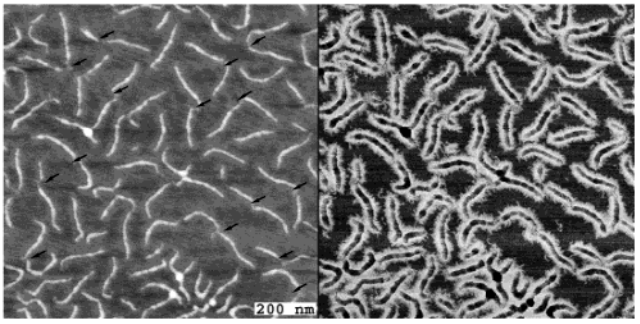

(a) (b)

Figure 7. AFM image of pODMA-*b*-p(BPEM-*g*-*n*BuA) brushes (cast from chloroform): (a) height (verical scale 5 nm); (b) phase (vertical scale 20°).

Figure 7 shows the AFM image of the pODMA-*b*-p(BPEM-*g*-*n*BuA) brushes, i.e., molecules with one pODMA tail. The white threads in the height image (Figure 7a) correspond to brush backbones dressed with desorbed side chains. Upon desorption, the p*n*BuA side chains segregate around the backbone and result in thickening of the backbone. This thickening enhanced the contrast in both height and phase images. In the height image (Figure 7a), the white color of the backbone is due to its 1 nm elevation relative to the substrate plane. In the phase image (Figure 7b), the darker areas correspond to lower phase shift relative to oscillations of the cantilever in air. Therefore, the darker color of the backbone is due to the relative softness of the bulk pBA compared to the monolayer of the side chains. One should note that at room temperature pBA is in liquid state.

The adsorbed side chains were clearly visualized only in the phase images as hairy white-colored shell around the black thread of the backbone. The half-width of the shell was measured to be 17 ± 2 nm, which is larger by a factor of 2 than the number-average length of the fully extended side chain with $DP_n = 35$. As discussed previously,[1] this discrepancy may be attributed to the polydispersity of the side chains. In this case, the longer side chains determine the shell width and the in-plane distance between adsorbed brush molecules.

Most of the molecules in Figure 7 associate by forming dimers (couples), which are indicated by arrows in Figure 7a. The coupling is consistent with the diblock copolymer structure of the backbone as shown in Scheme 3A.

The association behavior of the end-functionalized brushes was also investigated for p*n*BuA brushes with two pODMA ends, where chainlike structures or even networks might form. Figure 8 shows the height and phase images of the pODMA-*b*-p(BPEM-*g*-*n*BuA)-*b*-pODMA brush molecules adsorbed on mica. Similar to the images in Figure 7, both backbones and side chains were clearly visible in the height (Figure 8a) and phase (Figure 8b) images. We also attained clear of the pODMA tails as disklike patches at the brush ends. Their color, i.e., height, is intermediate between those

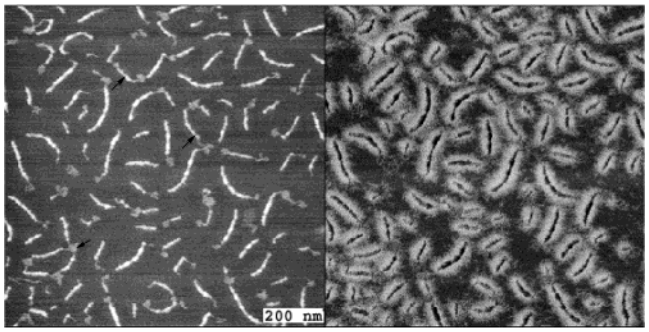

Figure 8. AFM image of pODMA-*b*-p(BPEM-*g*-*n*BuA)-*b*-pODMA brushes (cast from chloroform): (a) height (vertical scale 5 nm); (b) phase (vertical scale 50°).

Scheme 3. Aggregation of pODMA-*b*-p(BPEM-*g*-*n*BuA) (A) and pODMA-*b*-p(BPEM-*g*-*n*BuA)-*b*-pODMA (B) Molecular Brushes on Mica Surface

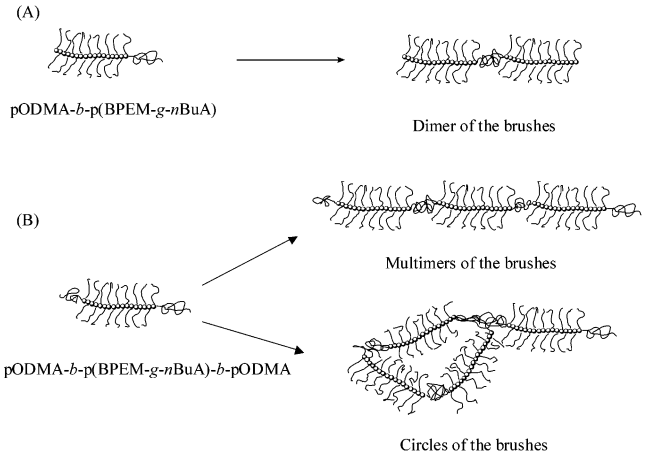

of the substrate and the backbone. Apparently, the disklike patches correspond to 2D coils of the pODMA tails, which are more flexible than the densely grafted p*n*BuA brushes. As expected, these molecules indeed form chainlike structures that consist of more than two molecules (Scheme 3B). Although most of the molecules in Figure 8 are single molecules, we also observed chains of 3 and chains of 4 molecules depicted by arrows in Figure 8a. Another typical structure was a ring of several molecules as depicted in the bottom-left corner in Figure 8a. To favor association, adsorption of the molecules with the hydrophobic pODMA tails were performed from acetone, a more polar solvent. As seen in Figure 9, the association became network-like. The pODMA linkage may accommodate more than two molecules and thus result in the network formation. DSC measurements indicate that bulk samples of both copolymer brushes show glass transition for the pBA side chains at 48 ± 1 °C and melting of PODMA at 25 ± 1 °C. The melting enthalpy was higher for the ABA block copolymer due to much higher content of the PODMA segments (ΔH = 3.7 J/g vs 0.5 J/g, respectively).

Conclusions

Well-defined macromolecular brushes with AB and ABA "block−graft" architectures were synthesized by ATRP using chain extension and "grafting from" methods. The synthesized pODMA-*b*-(pBPEM-*g*-*n*BuA) and pODMA-*b*-(pBPEM-*g*-p*n*BuA)-*b*-pODMA are of high molecular weight and relative low polydispersities. AFM demonstrated that the molecular brushes, adsorbed on the mica surface, have a wormlike structure. The pBPEM segment in the main chain was extended due to the strong interaction between the polar *n*BuA units and the polar mica substrate. The pODMA segments tended to aggregate strongly due to the van der Waals attraction of the pODMA chain ends and also due to crystallization of the relatively long C18 chains. Different morphologies can be formed on mica surface by using different solvents during the AFM samples preparation.

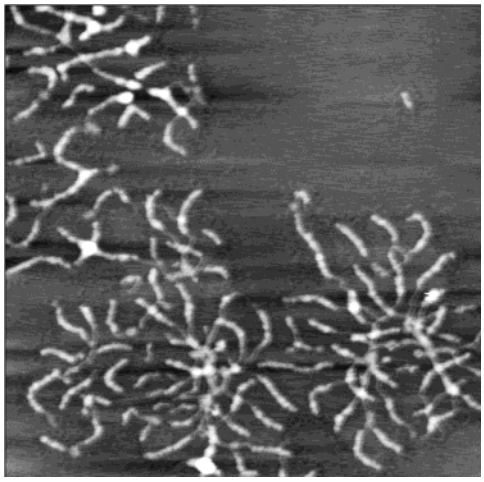

Figure 9. AFM image of pODMA-*b*-p(BPEM-*g*-*n*BuA)-*b*-pODMA brushes (cast acetone). Height (vertical scale 5 nm).

Acknowledgment. This work was financially supported by the National Science Foundation (ECS-01-03307) and CRP Consortium members at Carnegie Mellon University.

References and Notes

(1) Sheiko, S. S.; Moller, M. *Chem. Rev.* **2001**, *101*, 4099−4123.
(2) Tsukahara, Y.; Tsutsumi, K.; Yamashita, Y.; Shimada, S. *Macromolecules* **1990**, *23*, 5201−5208.
(3) Dziezok, P.; Sheiko, S. S.; Fischer, K.; Schmidt, M.; Moller, M. *Angew. Chem., Int. Ed. Engl.* **1997**, *36*, 2812−2815.
(4) Schappacher, M.; Deffieux, A. *Macromolecules* **2000**, *33*, 7371−7377.
(5) Meijs, G. F.; Rizzardo, E. *J. Macromol. Sci., Rev. Macromol. Chem. Phys.* **1990**, *C30*, 305−377.
(6) Matyjaszewski, K., Ed. *Controlled Radical Polymerization;* ACS Symp. Ser. 685; American Chemical Society: Washington, DC, 1998.
(7) Matyjaszewski, K., Ed. *Controlled/Living Radical Polymerization. Progress in ATRP, NMP, and RAFT;* ACS Symp. Ser. 768; American Chemical Society: Washington, DC, 2000.
(8) Matyjaszewski, K., Davis, T. P., Eds. *Handbook of Radical Polymerization*; John Wiley & Sons: New York, 2002.
(9) Davis, K. A.; Matyjaszewski, K. *Adv. Polym. Sci.* **2002**, *159*, 1−169.
(10) Wang, J. S.; Matyjaszewski, K. *J. Am. Chem. Soc.* **1995**, *117*, 5614−5615.
(11) Matyjaszewski, K.; Xia, J. H. *Chem. Rev.* **2001**, *101*, 2921−2990.
(12) Kamigaito, M.; Ando, T.; Sawamoto, M. *Chem. Rev.* **2001**, *101*, 3689−3745.
(13) Matyjaszewski, K. *Chem.—Eur. J.* **1999**, *5*, 3095−3102.
(14) Patten, T. E.; Matyjaszewski, K. *Acc. Chem. Res.* **1999**, *32*, 895−903.
(15) Patten, T. E.; Matyjaszewski, K. *Adv. Mater.* **1998**, *10*, 901−915.
(16) Beers, K. L.; Gaynor, S. G.; Matyjaszewski, K.; Sheiko, S. S.; Moller, M. *Macromolecules* **1998**, *31*, 9413−9415.
(17) Borner, H. G.; Beers, K.; Matyjaszewski, K.; Sheiko, S. S.; Moller, M. *Macromolecules* **2001**, *34*, 4375−4383.

(18) Borner, H. G.; Duran, D.; Matyjaszewski, K.; da Silva, M.; Sheiko, S. S. *Macromolecules* **2002**, *35*, 3387−3394.
(19) Cheng, G. L.; Boker, A. A.; Zhang, M. F.; Krausch, G.; Muller, A. H. E. *Macromolecules* **2001**, *34*, 6883−6888.
(20) Qin, S. H.; Börner, H. B.; Matyjaszewski, K.; Sheiko, S. S. *Polym. Prepr. (Am. Chem. Soc., Div. Polym. Chem.)* **2002**, *43* (2), 237−238.
(21) Neugebauer, D.; Matyjaszewski, K. *Polym. Prepr. (Am. Chem. Soc., Div. Polym. Chem.)* **2002**, *2002* (2), 241−242.
(22) Plate, N. A.; Shibaev, V. P.; Petrukhi, Bs.; Zubov, Y. A.; Kargin, V. A. *J. Polym. Sci., Polym. Chem. Ed.* **1971**, *9*, 2291−2298.
(23) Hsieh, H. W. S.; Post, B.; Morawetz, H. *J. Polym. Sci., Polym. Phys. Ed.* **1976**, *14*, 1241−1255.
(24) Inomata, K.; Sakamaki, Y.; Nose, T.; Sasaki, S. *Polym. J.* **1996**, *28*, 986−991.
(25) Yokota, K.; Hirabayashi, T.; Inai, Y. *Polym. J.* **1994**, *26*, 105−108.
(26) Beers, K. L.; Matyjaszewski, K. *J. Macromol. Sci., Pure Appl. Chem.* **2001**, *38*, 731−739.
(27) Qin, S. H.; Pyun, J.; Saget, J.; Matyjaszewski, K.; Jia, S. J.; Kowalewski, T. *Polym. Prepr. (Am. Chem. Soc., Div. Polym. Chem.)* **2002**, *43* (2), 235−236.
(28) Beers, K. L.; Boo, S.; Gaynor, S. G.; Matyjaszewski, K. *Macromolecules* **1999**, *32*, 5772−5776.
(29) Matyjaszewski, K.; Patten, T. E.; Xia, J. H. *J. Am. Chem. Soc.* **1997**, *119*, 674−680.
(30) Matyjaszewski, K.; Shipp, D. A.; Wang, J. L.; Grimaud, T.; Patten, T. E. *Macromolecules* **1998**, *31*, 6836−6840.
(31) Shipp, D. A.; Wang, J. L.; Matyjaszewski, K. *Macromolecules* **1998**, *31*, 8005−8008.
(32) Sheiko, S. S.; Prokhorova, S. A.; Beers, K. L.; Matyjaszewski, K.; Potemkin, I. I.; Khokhlov, A. R.; Moller, M. *Macromolecules* **2001**, *34*, 8354−8360.

MA021472W